

# Binary fission-fragment yields from the reaction $^{251}\text{Cf}(n_{\text{th}}, f)$

E. Birgersson<sup>\*†</sup>, S. Oberstedt<sup>\*</sup>, A. Oberstedt<sup>†</sup>, F.-J. Hamsch<sup>\*</sup>,  
D. Rochman<sup>¶</sup>, I. Tsekhanovitsch<sup>‡</sup>

<sup>\*</sup>EC-JRC IRMM, B-2440 Geel, Belgium,

<sup>†</sup>Dept. of Natural Sciences, Örebro University, SE-70182 Örebro, Sweden

<sup>¶</sup>Brookhaven National Laboratory, National Nuclear Data Center (NNDC), USA

<sup>‡</sup>ILL, F-38042 Grenoble Cedex, France

**Abstract.** The recoil mass spectrometer LOHENGRIN of the Laue-Langevin Institute, Grenoble has been used to measure the light fission-fragment mass yield and kinetic energy distributions from neutron-induced  $^{252}\text{Cf}^*$ , using  $^{251}\text{Cf}$  as target material.

**Keywords:** Californium-251, neutron-induced fission, fission fragment spectroscopy.

**PACS:** 25.85.Ec, 28.20.-v, 29.30.Ep, 24.75.+i

## INTRODUCTION

The interpretation of fission-fragment properties in terms of so-called fission modes has been successfully applied in the actinide region to describe mass yield and total kinetic energy distributions as a function of incident neutron energy. From investigating fission-fragment characteristics as a function of excitation energy the mass-asymmetric standard I (S1) and standard II (S2) modes as well as the mass-symmetric super-long (SL) mode have been used to consistently describe the mass- and total kinetic energy (TKE) distributions [1-4]. In case of spontaneous fission of  $^{252}\text{Cf}$ , which is considered as standard reaction in nuclear fission, the number of traditional fission modes is not sufficient to properly describe the experimentally obtained fission-fragment distributions. Additional theoretically obtained fission modes have to be included into the analysis to improve the description of the data. In order to achieve experimental confirmation of the number of fission modes present in  $^{252}\text{Cf}$  the fission-fragment properties and mean kinetic energies were measured for the reaction  $^{251}\text{Cf}(n_{\text{th}}, f)$  at thermal excitation.

## EXPERIMENT

The experiment was performed at the recoil mass spectrometer LOHENGRIN of the Institute Laue-Langevin. The target consisted of  $\text{Cf}_2\text{O}_3$  deposited on a titanium backing. The active spot had a diameter of 4 mm and a thickness of  $87.7 \mu\text{g}/\text{cm}^2$ . The initial isotopic composition of the californium batch was the following:  $^{249}\text{Cf}$  (18 %),

CP798, *Nuclear Fission and Fission-Product Spectroscopy*,

edited by H. Goutte, H. Faust, G. Fioni, and D. Goutte

© 2005 American Institute of Physics 0-7354-0288-4/05/\$22.50

$^{250}\text{Cf}$  (35 %),  $^{251}\text{Cf}$  (46 %) and  $^{252}\text{Cf}$  (1 %). In order to avoid loss of material due to sputtering, when the target is heated in the high thermal neutron flux of  $5 \cdot 10^{14}$  neutrons/cm<sup>2</sup>/s, the target was covered by a 0.25  $\mu\text{m}$  thick nickel foil. The nickel foil is supported by an acrylic layer, which is supposed to evaporate before the measurements starts.

In LOHENGRIN the separation of fission-fragments is done according to their  $A/q$  and  $E/q$  ratios, where  $A$ ,  $E$  and  $q$  are the mass number, kinetic energy and ionic charge state of the fission fragments, respectively. The fission fragments are detected after separation with an ionisation chamber, which has a segmented anode to serve as a  $\Delta E$ - $E$  telescope.

## MEASUREMENTS AND DATA ANALYSIS

The emission yield  $Y(A)$  of a fission fragment of mass  $A$  is determined according to:

$$Y(q, E) = \frac{Y(A)}{\sqrt{2\pi}\sigma_E} e^{-\frac{(E-\langle E \rangle)^2}{2\sigma_E^2}} \frac{1}{\sqrt{2\pi}\sigma_q} e^{-\frac{(q-\langle q(E) \rangle)^2}{2\sigma_q^2}}, \quad (1)$$

where  $\langle q(E) \rangle$  is the mean ionic charge as a function of energy and calculated according to Ref. [5] but with parameters refitted using the experimental results. For each mass an energy distribution at the mean ionic charge was measured and at the mean kinetic energy an ionic charge distribution was measured. However several corrections have to be made to the raw data before yield and kinetic energy may be determined.

Due to the high neutron-induced reaction cross-sections for  $^{251}\text{Cf}$  and the extremely high neutron flux the decrease of target material, the so-called burn-up, has to be taken into account and monitored. This was done by measuring mass  $A = 100$  at ionic charge  $q = 22$  and kinetic energies  $E_k = 80$  to  $115$  MeV in steps of  $5$  MeV several times per day. The resulting intensity and mean kinetic energies for the different burn-up measurements as a function of time is shown in Fig. 1. The burn-up is described in the usual way by a two-exponential function, where the fast component accounts for material losses during initial heating of the target. As it may be depicted from Fig. 1 the burn-up data show quite some structure, which has to be attributed to drifts in the electric field between the condenser plates of LOHENGRIN. However, based on only those burn-up runs performed directly after each day formation, performed on the electronic condenser plates, proper corrections to these instabilities could be established. Eventually, all burn-up measurements were used to correct the raw data for the electronic instabilities.

The increase in mean kinetic energy, see right part of Fig. 1, is described by a two exponential, where one of the time constants is given the same value as in another experiment performed at LOHENGRIN on  $^{245}\text{Cm}$  which had a similar fission rate [6]. The initial strong increase of the mean kinetic energy is due to the acrylic layer on the nickel foil, which is supposed to evaporate before starting the experiment. Since this foil was mounted upside down at ILL, the acrylic layer evaporated much slower. The function describing the increase in kinetic energy as shown in Fig. 1 was used to estimate the kinetic energy at  $t = 0$ , when the target properties were known. Energy

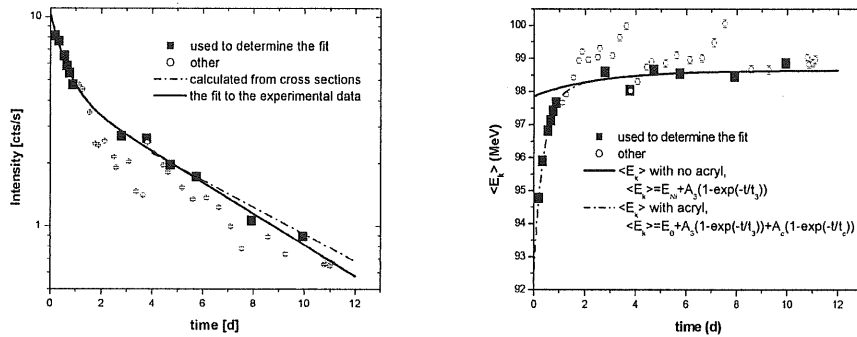


**FIGURE 1. Left:** Burn-up measurements performed to monitor the decrease of fissile material. The fit is based on the squares. The open circles and the squares are used to monitor electronic drifts. **Right:** The increase in mean kinetic energy described by a two-exponential is based on the squares. The open circles and squares are used to monitor the electronic drifts. Also shown is the one-exponential with time dependence according to Ref. [6].

losses in the target and the Ni-foil were then calculated using SRIM2003 [7].

The composition of the target changes during the experiment. At the end of the experiment 25% of the fission-fragments come from  $^{249}\text{Cf}$ . The other isotopes contribute to less than 10% and are not taken into account. Therefore a correction to the burn-up function was made since it was measured at  $A = 100$  and the relative contributions from  $^{249}\text{Cf}$  and  $^{251}\text{Cf}$  are not the same. Once these corrections to the obtained data have been performed the extraction of the contribution from the  $^{249}\text{Cf}$  can be calculated. The relative mass yield of  $^{251}\text{Cf}$  is given by

$$y_1(A) = \frac{Y(A)}{f_1(t(A))} \cdot \frac{1 + \sum_{A'=80}^{124} \frac{f_9(t(A'))}{f_1(t(A'))} y_9(A')}{\sum_{A'=80}^{124} \frac{Y(A')}{f_1(t(A'))}} - \frac{f_9(t(A))}{f_1(t(A))} y_9(A), \quad (2)$$

where  $f_1(t(A))$  and  $f_9(t(A))$  are describing the fission fragments coming from  $^{251}\text{Cf}$  and  $^{249}\text{Cf}$ , respectively, and  $f_1(t(A)) + f_9(t(A)) = 1$ . The  $y_1(A)$  and  $y_9(A)$  are the relative mass yield for  $^{251}\text{Cf}$  and  $^{249}\text{Cf}$ , respectively.  $Y(A)$  is the burn-up corrected yield.

## RESULTS AND DISCUSSION

The obtained post-neutron fission-fragment distribution of  $^{252}\text{Cf}^*$  at thermal excitation is shown (square symbol) in Fig. 2 together with an evaluation from Ref. [8] and data from the spontaneous fission of  $^{252}\text{Cf}$  [9]. The data from the fission at thermal excitation are in good agreement with the evaluation. The distribution appears to be broader than in the case of spontaneous fission. For a more realistic comparison the LOHENGRIN data have been 5-point smoothed to mimic the resolution of the SF data measured with the 2E-technique. The emission yields around  $A = 115$  is enhanced and diminished around  $A = 105$ . In terms of fission modes the more compact standard I mode seems to be enhanced compared to the more deformed mode standard II. This should lead to an increase of the mean kinetic energy for the mass region above  $A =$

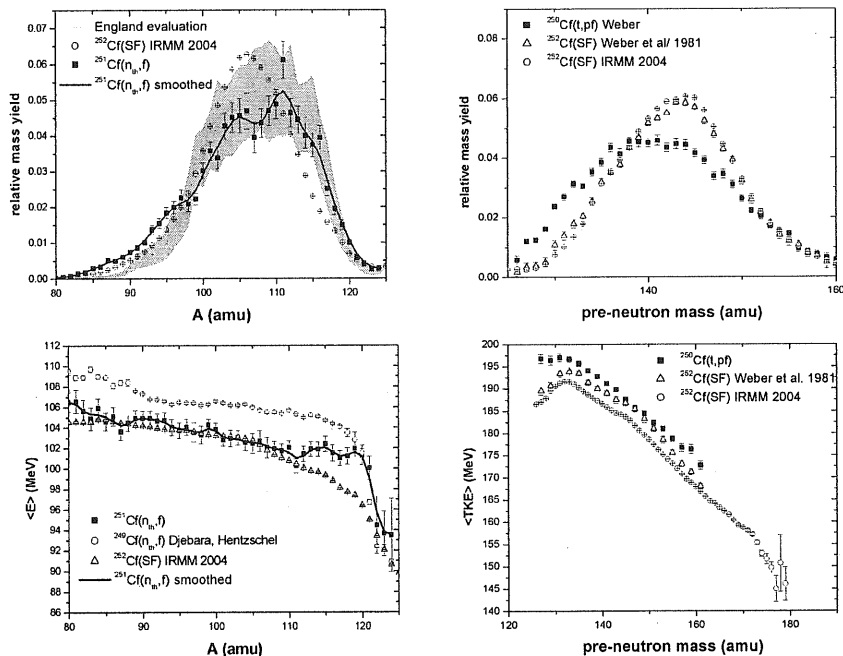


**FIGURE 2.** Top-left: Light fission-fragments mass distribution from thermal neutron induced fission of  $^{252}\text{Cf}^*$  (squares) compared to an evaluation from Ref. [8], where the grey-shaded area indicates lower and upper limits. Circles are data from the spontaneous fission of  $^{252}\text{Cf}$  [9]. Top-Right: Heavy pre-neutron fission-fragment mass distribution from the fission of  $^{252}\text{Cf}^*$  (squares, [10]) following the reaction  $^{250}\text{Cf}(t, p)$  together with data from the spontaneous fission of  $^{252}\text{Cf}$  (open symbols, [9,10]). Bottom-left: Mean kinetic energy as a function of the fission-fragment mass A:  $^{251}\text{Cf}(n_{th}, f)$  (squares, this work),  $^{249}\text{Cf}(n_{th}, f)$  (circle [11,12,13]) and  $^{252}\text{Cf}(\text{SF})$  (triangles, [9]). Bottom-Right: Total kinetic energy (TKE) as a function of the fission-fragment mass prior to prompt neutron emission [9, 10].

110, which is indeed the case (Fig. 2, lower part). This observation confirms findings in Ref. [10] using the reaction  $^{250}\text{Cf}(t, p)$  at a slightly higher mean excitation energy.

## REFERENCES

1. P. Siegler, F.-J. Hamsch, S. Oberstedt, J. P. Theobald, Nucl. Phys. **A594** 45 (1995)
2. S. Oberstedt, F.-J. Hamsch, F. Vives, Nucl. Phys. **A644** 289 (1998)
3. F. Vivès, F.-J. Hamsch, H. Bax, S. Oberstedt, Nucl. Phys. **A662** 63 (2000)
4. F.-J. Hamsch, F. Vivès, P. Siegler, S. Oberstedt, Nucl. Phys. **A679** 3 (2000)
5. V. S. Nikolaev, and Dmitriev, *Physics Letters* **28A**, 277-278 (1968).
6. T. Friedrichs, *PhD thesis*, Braunschweig: unpublished (1998).
7. Computer code SRIM 2003.26, available from J.F. Ziegler, IBM Research, Yorktown, NY-10598, USA and J. P. Biersack, Hahn-Meitner Institut, 1 Berlin 39 (2003)
8. T. R. England, and B. F. Rider, *LA-UR-94-3106, ENDF-349* (1994).
9. F.-J. Hamsch, *Private communication* (2004).
10. J. Weber, H. C. Britt, and J. B. Wilhelmy, *Phys. Rev.* **C23**, 2100 (1981).
11. M. Djebara et al., *Nucl. Phys* **A496**, 346 (1989).
12. R. Hentzschel, *Nucl. Phys* **A571**, 427 (1994).
13. R. Hentzschel, *PhD thesis*. Mainz University: unpublished (1992).